

## Supplementary Information

### **Anomalous atmospheric circulation favored the spread of COVID-19 in Europe**

A. Sanchez-Lorenzo<sup>1</sup>, J. Vaquero-Martínez<sup>1</sup>, J. Calbó<sup>2</sup>, M. Wild<sup>3</sup>, A. Sartuntún<sup>4</sup>,  
J.A. Lopez-Bustins<sup>5</sup>, J.M. Vaquero<sup>1</sup>, M. Antón<sup>1</sup>

<sup>1</sup> Department of Physics, University of Extremadura, Badajoz, Spain

<sup>2</sup> Department of Physics, University of Girona, Girona, Spain

<sup>3</sup> Institute for Atmosphere and Climate (IAC), ETH Zurich, Zurich, Switzerland

<sup>4</sup> Unit of Legal Medicine, Department of Physiology and Pharmacology, University of Cantabria, Santander, Spain

<sup>5</sup> Climatology Group, Department of Geography, University of Barcelona, Barcelona, Spain

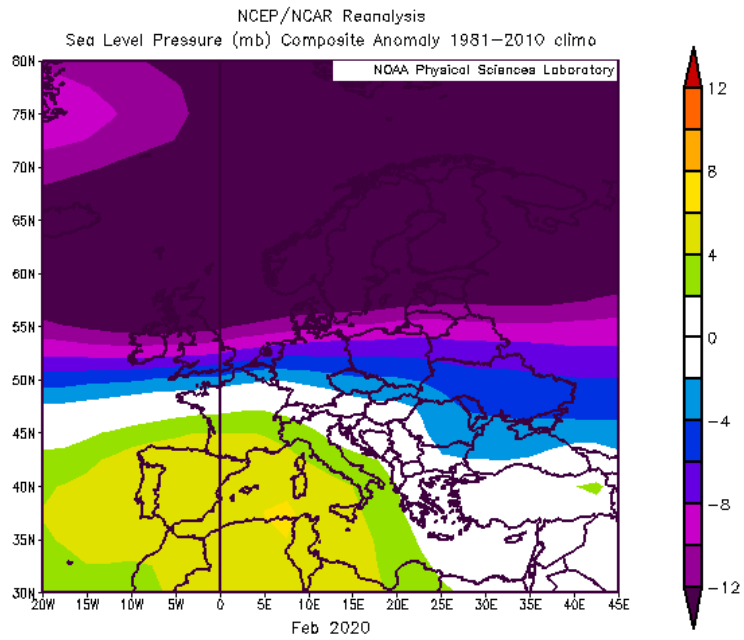


Figure S1. Anomaly pattern of sea level pressure (mb) for February 2020 over Europe as compared to the climatology mean (1981-2010 period). Image generated with the Web-based Reanalysis Intercomparison Tool provided by the NOAA/ESRL Physical Sciences Laboratory, Boulder Colorado from their Web site at <http://psl.noaa.gov/>

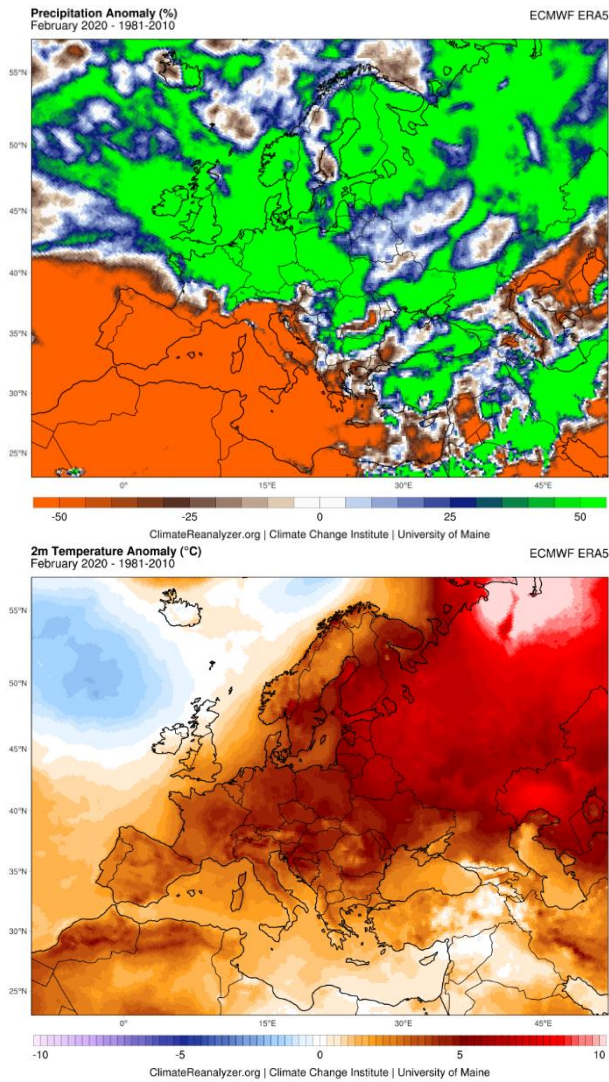


Figure S2. Anomaly pattern of (top) precipitation (in %) and (bottom) 2-m temperature (in °C) during February 2020 as compared to the climatology mean (1981-2010 period). Image generated with Climate Reanalyzer, Climate Change Institute, University of Maine, USA (<https://ClimateReanalyzer.org>).

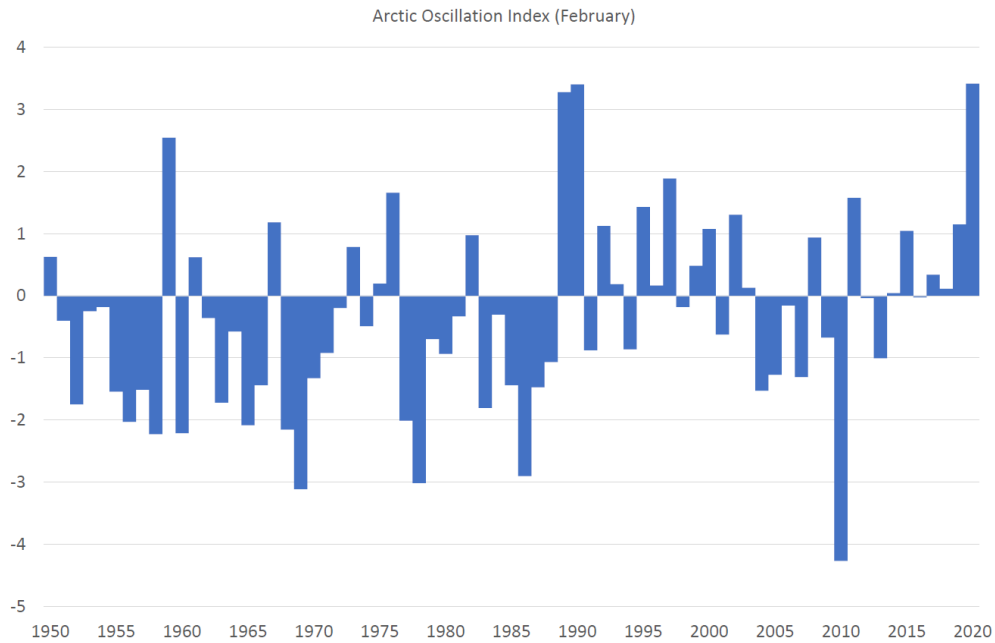


Figure S3. Time series of the Arctic Oscillation (AO) index from 1950 to 2020 provided by the Climate Prediction Center of the National Oceanic and Atmospheric Administration (NOAA). The February 2020 is the highest value (3.417), closely followed by 1990 (3.402) and 1989 (3.279) and far away from the 4<sup>th</sup> largest value in 1959 (2.544). This highlights the exceptionally extreme AO pattern of the past February 2020 in a long-term perspective.



Figure S4. Location of the 15 countries used in this study that provided cases and deaths of COVID-19.



Figure S5. Location of the autonomous communities of Spain, as well as the two autonomous cities of Ceuta and Melilla. The Canary Islands has not been included in this study due to its geographical location in tropical latitudes.

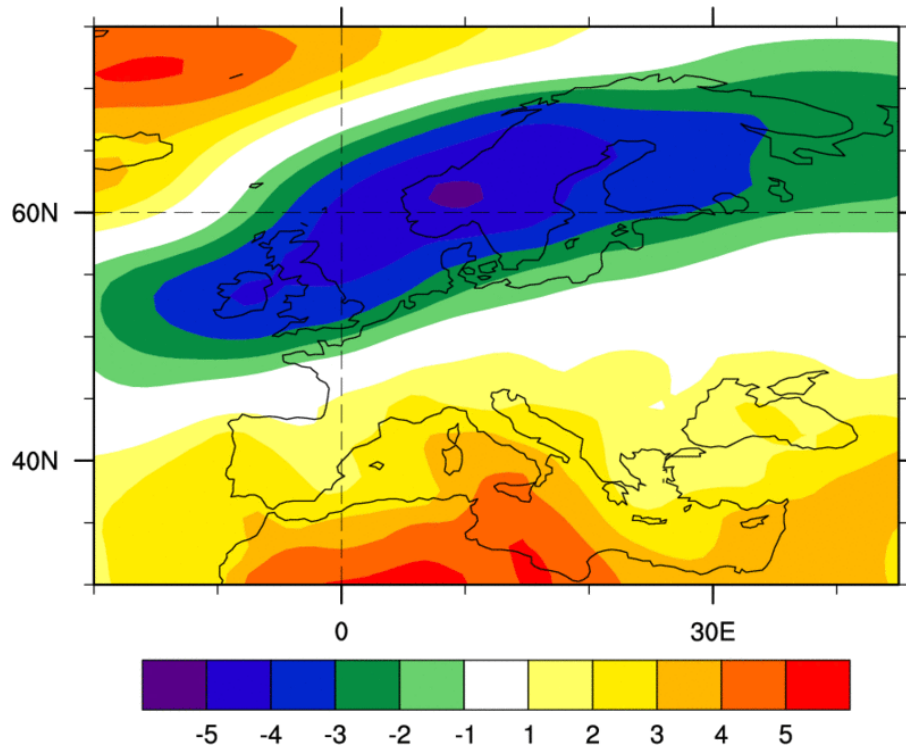


Figure S6. Anomaly map of the sea level pressure (SLP) field extracted from ERA20C reanalysis of September and October 1918 as compared to the climatological mean (1981-2010 period). Image generated with the Web-based Reanalysis Intercomparison Tool provided by the NOAA/ESRL Physical Sciences Laboratory, Boulder Colorado from their Web site at <http://psl.noaa.gov/>

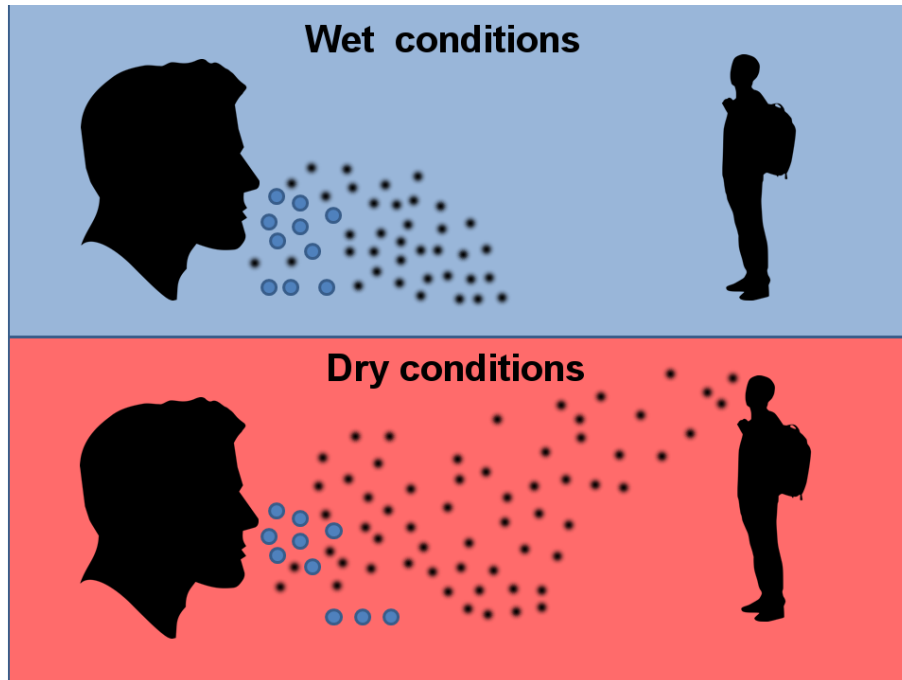


Figure S7. Schematic representation of particles emitted by a cough, with the large droplets settled down nearby (e.g., 1 m distance) and the smaller airborne particles spreading in suspension for longer time, and reaching longer distances, especially in dry and stable conditions as compared to wet environments. It is also possible that a resuspension of aerosol particles can eventually happen due to human activities (e.g., walking, cleaning, etc.) or air flows, which is enhanced under dry conditions due to the lack of precipitation.



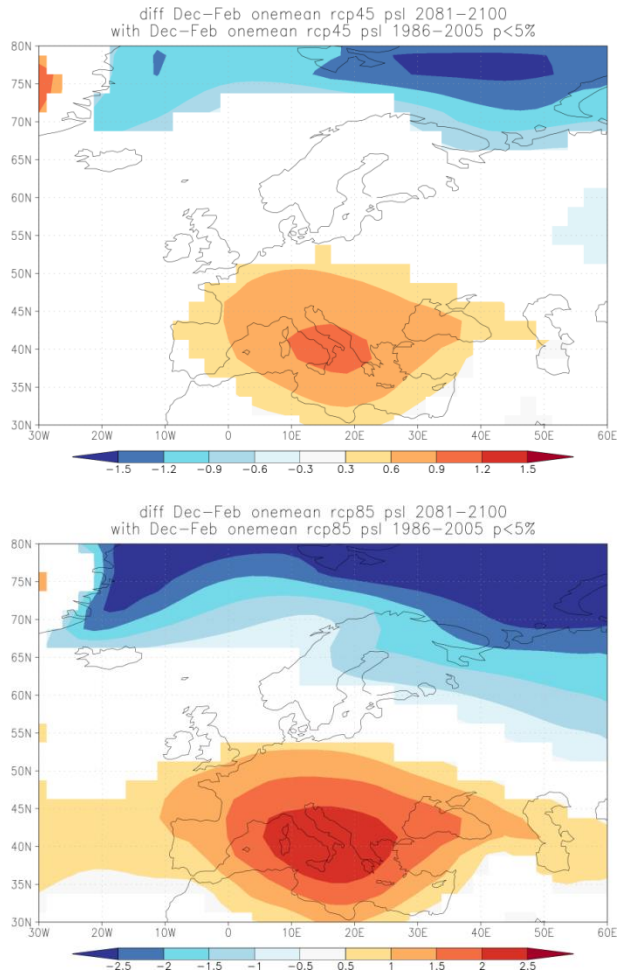


Figure S8. Winter (DJF) anomalies of sea level pressure (SLP, in mb) as computed for the CMIP5 ensemble (one member per model) for the (top) RCP4.5 and (bottom) RCP8.5 emission scenarios at the end of the 21st century. The differences are computed expressed as the 2081-2100 minus 1986-2005 period. Only statistically significant fields ( $p < 0.05$ ) are plotted as estimated by a Student's t-Test. Map composed with the data and tools provided by the KNMI Climate Explorer website (<https://climexp.knmi.nl/start.cgi>). The maps show a consistent picture of an intensification of the positive NAO phase, which implies that in the future winter conditions as experienced over Europe past February 2020 could become more common.